ADVANCES IN NUCLEAR SCIENCE AND APPLICATIONS

Volume 2, No. 2 (2026), P. 111-120

Investigation of the nuclear modification factor for inclusive charged particles in Au+Au collisions within the BES-II STAR energy range using the UrQMD and SMASH+vHLLE models

A.Zh. Aitbayev[1,2,3], A.A. Aparin[1],
A.A. Korobitsin[1], Ye.S. Mukhamedzhanov[1,3]

[1]Joint Institute for Nuclear Research, Dubna, Russia

[2]Al-Farabi Kazakh National University, Almaty, Kazakhstan

[3]Institute of Nuclear Physics, Almaty, Kazakhstan

e-mail: a.ali.970424@gmail.com

DOI: 10.63907/ansa.v2i2.90
Received: 9 June 2026

Abstract

The Beam Energy Scan (BES) program at the RHIC collider is designed to perform a detailed study of the QCD phase diagram, including the search for the phase transition boundary of the first-order phase transition from hadronic matter to QGP, the determination of the QCD critical point location, and the investigation of other aspects of the phase behavior of nuclear matter. A previously observed feature in QGP studies is the suppression of high-transverse-momentum particle yields, $p_T > 2$ GeV/c, at $\sqrt{s_{NN}} = 62.4$–200 GeV. This effect was established through measurements of the nuclear modification factors R_{AA} and R_{CP} for charged particles in the BES-I program of the STAR experiment (Phys. Rev. Lett. **121**, 032301 (2018)). This work presents a comparison of the nuclear modification factor R_{CP} for inclusive charged particles in $Au+Au$ collisions at $\sqrt{s_{NN}} = 7.7-27$ GeV, obtained from Monte Carlo simulations using the UrQMD transport model and the SMASH+vHLLE hybrid model, with the published experimental data from the STAR BES-I program. The ability of the models under consideration to reproduce the experimental observations over a wide range of energies and transverse momenta is analyzed, and possible sources of the observed discrepancies are discussed.

1 Introduction

Ultra-relativistic heavy-ion collisions create extreme conditions of temperature and energy density, in which ordinary hadronic matter undergoes a transition to a state of deconfined quarks and gluons — the quark-gluon matter (QGM) [1–4]. This state of strongly interacting partonic matter is predicted by quantum chromodynamics (QCD) [5] and was experimentally discovered at the Relativistic Heavy Ion Collider (RHIC). Currently, studies of this state continue at RHIC, the Super Proton Synchrotron (SPS), and the Large Hadron Collider (LHC). Determining the properties of QGM and searching for the critical point on the QCD phase diagram remain among the key challenges in modern heavy-ion physics.

The QCD phase diagram describes the state of matter as a function of temperature (T) and baryon chemical potential (μ_B) [6]. In heavy-ion collision experiments, these parameters can be varied by changing the collision energy: high energies correspond to small values of μ_B , while decreasing the energy leads to an increase in the baryon chemical potential. Lattice QCD calculations predict a smooth crossover transition at small μ_B [7, 8], whereas at sufficiently large μ_B , a first-order phase transition is expected [9, 10]. The endpoint of this phase transition line corresponds to the QCD critical point.

To experimentally investigate the phase structure of nuclear matter over a wide range of temperatures and baryon chemical potentials, the Beam Energy Scan (BES) program was initiated at RHIC. Its strategy consists of systematically varying the collision energy of heavy ions, which allows the creation of systems with different initial thermodynamic conditions and enables the tracking of their evolution trajectories on the $T-\mu_B$ plane. This approach provides the opportunity to explore different regions of the phase diagram and to search for the location of the first-order phase transition boundaries and the critical point.

One of the most sensitive tools for studying the properties of the hot and dense medium produced in heavy-ion collisions is jet quenching — the phenomenon of energy loss experienced by high-energy partons traversing a dense QGM medium [11–15]. Partons produced in primary interactions with large transverse momentum (p_T) propagate through the dense medium and lose energy. As a result, a suppression of hadron yields at high transverse momentum (p_T) is observed. The observation of such suppression at RHIC became one of the most important pieces of evidence for the formation of a dense medium in a deconfined state with pronounced collective properties.

Quantitatively, the contribution of nuclear modification to particle production in ion collisions can be characterized by the nuclear modification factor R_{CP} . It is defined as the ratio of particle yields in central and peripheral collisions, normalized by the average number of binary nucleon-nucleon collisions $\langle N_{coll}\rangle$ in the corresponding centrality classes:

$$R_{CP} = \frac{\langle N_{\rm coll}\rangle_{\rm peripheral}}{\langle N_{\rm coll}\rangle_{\rm central}} \cdot \frac{\left(\dfrac{d^2N}{dp_T\,d\eta}\right)_{\rm central}}{\left(\dfrac{d^2N}{dp_T\,d\eta}\right)_{\rm peripheral}} \tag{1}$$

where η is the pseudorapidity; $\langle N_{\rm coll}\rangle_{\rm central}$ and $\langle N_{\rm coll}\rangle_{\rm peripheral}$ are the average numbers of binary nucleon-nucleon collisions for central and peripheral events,

respectively; $\frac{d^2N}{dp_T\,d\eta}$ is the differential particle yield spectrum.

The values of $\langle N_{\text{coll}} \rangle$ for given centrality classes are typically estimated using the Monte Carlo Glauber model. In the absence of nuclear medium effects, a heavy-ion collision could be considered as a simple superposition of independent nucleon-nucleon interactions, which would yield $R_{CP} = 1$ over the entire p_T range. Deviations from unity indicate the influence of the nuclear medium: values of $R_{CP} < 1$ correspond to suppression, while $R_{CP} > 1$ correspond to enhancement of particle production.

In the intermediate transverse momentum region $p_T \approx 1$ GeV/c, the observed nuclear modification factor is affected by competing physical processes. Enhancement of the yield may be associated with the Cronin effect, radial collective flow, or coalescence mechanisms [16], which shift the particle spectrum toward higher p_T. At the same time, energy loss due to propagation through the dense medium leads to a redistribution of energy of high-momentum partons and, consequently, to suppression of hadron yields at high p_T. Thus, the measured R_{CP} reflects a balance between these competing mechanisms, and values exceeding unity in a certain transverse momentum range do not exclude the possibility of QGP formation.

During the first phase of the BES program (BES-I) at the STAR experiment, the nuclear modification factor was measured for inclusive charged particles in Au+Au collisions over a wide energy range. A gradual change in the behavior of R_{CP} was observed — from a dominance of enhancement effects at low energies to pronounced suppression at higher energies, indicating a change in the properties of the produced medium. In this work, we present a comparison of the nuclear modification factors R_{CP} obtained from UrQMD and SMASH+vHLLE with the experimental R_{CP} data from the BES-I program. Figure 1 shows the R_{CP} measurements previously obtained by the STAR experiment from the BES-I data. It can be seen from Fig. 1 that the available statistics at low energies do not allow a definitive conclusion regarding the behavior of particles at high transverse momenta.

2 Monte Carlo Generators for Modeling Heavy-Ion Collisions

For the theoretical description and interpretation of experimental data on heavy-ion collisions, Monte Carlo methods based on microscopic transport and hybrid models are widely used. In this work, simulations of Au+Au collisions at $\sqrt{s_{NN}} =$ 7.7, 9.2, 11.5, 14.5, 17.3, 19.6, and 27 GeV are performed using two approaches: the UrQMD transport model and the SMASH+vHLLE hybrid model.

2.1 Microscopic Modeling of Hadronic Interactions: UrQMD

One of the most widely used tools for simulating nucleus-nucleus collisions over a broad energy range is the UrQMD (Ultra-relativistic Quantum Molecular Dynamics) model [17, 18]. It implements a microscopic transport approach and allows the dynamics of the nuclear system to be traced at the level of individual hadrons and resonances.

Within UrQMD, complex interactions are described through a decomposition

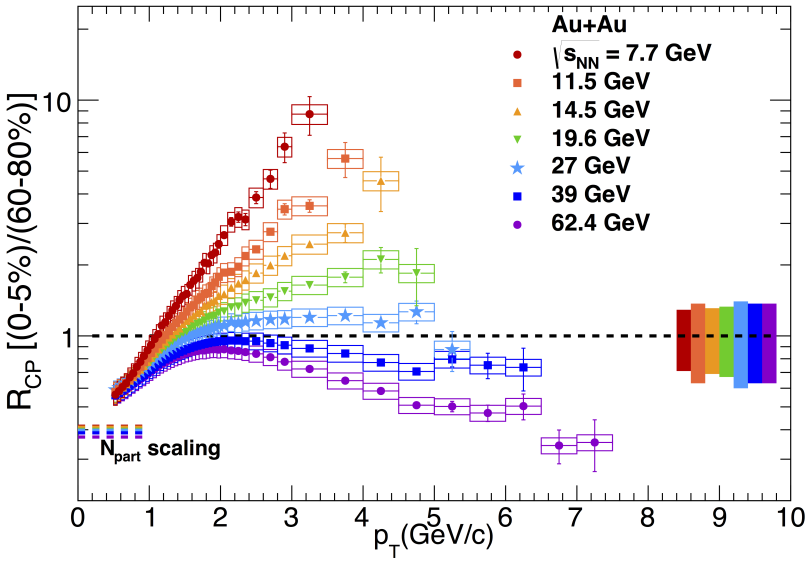

Figure 1: Nuclear modification factor R_{CP} for unidentified charged hadrons from the BES-I program at RHIC and at high collision energies. The uncertainty bands at unity on the right side of the plot correspond to the p_T-independent normalization uncertainty on N_{coll}; the color of the band matches the color of the data points for the corresponding energy. The vertical error bars represent statistical uncertainties, while the rectangular boxes represent systematic uncertainties. [16]

into a set of binary collisions, followed by the formation of excited states, resonance decays, and the formation and fragmentation of quark-gluon strings. The model includes an extended set of degrees of freedom — more than 50 baryon and 45 meson states — and strictly conserves baryon number, electric charge, and energy-momentum.

The mechanisms of particle production in the model depend on the collision energy. At $\sqrt{s_{NN}} \lesssim 5$ GeV, resonant processes followed by decays of excited states dominate. With increasing energy, the excitation of strings and their subsequent hadronization become increasingly important. The predictive power of UrQMD has been validated through numerous comparisons with experimental data: the model satisfactorily reproduces particle spectra, multiplicities, and interaction cross sections over the energy range from SIS ($\sqrt{s_{NN}} \approx 2$ GeV) up to the maximum RHIC energies ($\sqrt{s_{NN}} = 200$ GeV) [17, 19].

In this work, UrQMD version 3.4 was used in the hadronic cascade mode, without employing the effective potential field calculation. The impact parameter range for event simulation was taken to be 0–16 fm; default parameters recommended by the model developers were applied. UrQMD has been previously used successfully for the analysis of collective effects, including the study of elliptic flow and its fluctuations in various energy regimes, including in combination with hydrodynamic modules [20].

2.2 The SMASH+vHLLE Hybrid Approach

An alternative approach to describing the dynamics of heavy-ion collisions is based on the use of hybrid models, which combine a transport description of the initial and final stages with the addition of a relativistic hydrodynamic stage to simulate

the phase of highest energy density evolution. In this work, the SMASH+vHLLE hybrid model (version 2.1.3) was employed.

This approach is aimed at correctly describing regions of the QCD phase diagram at finite baryon density, where phase transitions are observed and the influence of the critical point may occur [21]. The evolution of the system in the model is divided into four sequential stages:

- The initial non-equilibrium stage, modeled by the SMASH transport code;
- The hydrodynamic evolution of the dense medium, implemented within the framework of viscous relativistic hydrodynamics (vHLLE);
- The transition from hydrodynamic variables to hadronic degrees of freedom (hadronization and particle sampling procedure, implemented via the Cooper-Frye method);
- The hadronic afterburner stage, in which SMASH describes the late-stage hadronic rescatterings.

For the energies $\sqrt{s_{NN}} = 7.7$ and 27 GeV, different values of the specific shear viscosity (η/s) were used in the hydrodynamic module — 0.20 and 0.12, respectively, as listed in Table 1. The spatial grid parameters and the smearing widths in the transverse and longitudinal directions are also given. It should be noted that in the current version of the calculations, the bulk viscosity was set to zero in the hadronization procedure; the values of other parameters were used unchanged.

Table 1: Parameters of the SMASH+vHLLE hybrid model (version 2.1.3) used for simulations of Au+Au collisions at $\sqrt{s_{NN}} =$ 7.7–27.0 GeV.

Parameter	**7.7**	**9.2**	**11.5**	**14.5**	**17.3**	**19.6**	**27.0**
Initial conditions							
Impact parameter b [fm]							
Central (0-5%)				$b \in [0, 3.3]$			
Peripheral (60-80%)				$b \in [11.4, 13.2]$			
Hydrodynamic stage							
Spatial grid ($n_x \times n_y \times n_z$)				$201 \times 201 \times 401$			
Specific shear viscosity η/s	0.20	0.19	0.18	0.17	0.16	0.15	0.12
Gaussian smearing R_g [fm]	1.40	1.30	1.10	1.20	1.15	1.1	1.0
Longitudinal smearing R_{gz} [fm]	1.2	1.1	1.0	0.9	0.8	0.7	0.4

3 Methodology for Calculating the Nuclear Modification Factor on Model Data

For a correct comparison of the simulation results with the experimental measurements of the STAR collaboration, the procedure for event and track selection used in calculating the nuclear modification factor R_{CP} in the UrQMD and SMASH+vHLLE models was made as close as possible to the analysis of experimental data, where feasible.

3.1 Definition of Centrality Classes in Model Calculations

Collision centrality is a key parameter in the calculation of R_{CP}, since it determines the initial size of the overlap region of the colliding nuclei and, consequently, the density of the subsequently formed medium. In experimental conditions, centrality is usually determined indirectly, for example, from the charged particle multiplicity. In model calculations, where complete information on the collision geometry is available, event classification by centrality was performed based on the impact parameter b.

To establish the correspondence between the impact parameter and the centrality classes (in percent of the total interaction cross section) traditionally used in experiment, the number of participants N_{part} and the number of binary nucleon-nucleon collisions N_{coll} were estimated for the Au+Au system. The calculation was performed using the standard toolkit for the optical Glauber model, available at [22]. The distributions obtained from geometrical considerations allowed us to establish the threshold values of the impact parameter that delineate different centrality intervals.

Figure 2 shows, as an example, the distribution of events as a function of the impact parameter for the Au+Au system at $\sqrt{s_{NN}} = 27$ GeV, with the boundaries corresponding to the selected centrality classes indicated. The vertical lines mark the intervals corresponding to central (0-5%) and peripheral (60-80%) collisions, which were subsequently used in constructing the nuclear modification factor R_{CP}. A similar procedure was applied for the other collision energies.

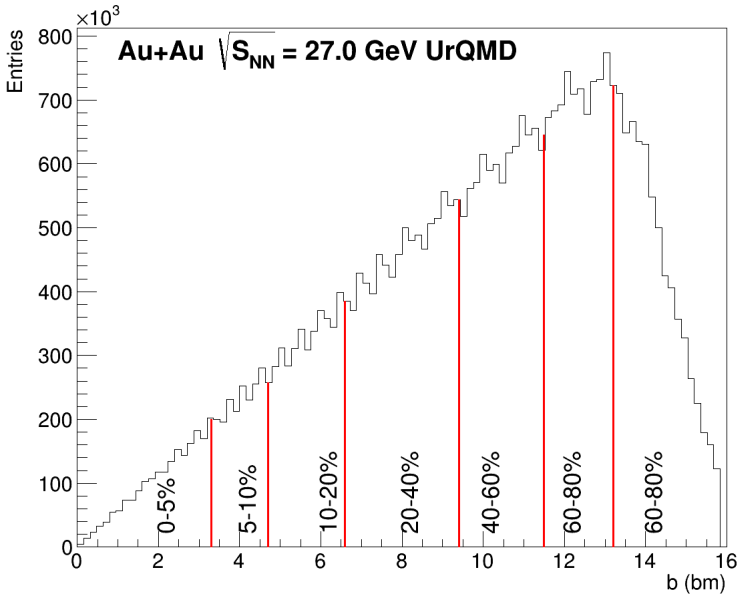

Figure 2: Distribution of events as a function of impact parameter in Au+Au simulations at $\sqrt{s_{NN}} = 27$ GeV. Vertical lines indicate the intervals corresponding to different centrality classes.

4 Simulation Results and Comparison with Experimental Data

This section presents the results of the calculation of the nuclear modification factor R_{CP} for charged particles, obtained using two different approaches to modeling heavy-ion collisions: the UrQMD transport model and the SMASH+vHLLE hybrid model. A comparison of the model predictions with the experimental data from the STAR collaboration, obtained during the first phase of the Beam Energy Scan program, is performed.

4.1 Methodological Aspects of the Comparison

To ensure a correct comparison of model and experimental results, a unified procedure for calculating the nuclear modification factor was applied in accordance with Eq. (1). The values of the average number of binary collisions $\langle N_{coll} \rangle$, obtained from Glauber model calculations, were used identically for both the experimental data analysis and the construction of the model dependences. In the present work, we adhere to the methodology employed in the BES-I program, which ensures methodological continuity and comparability of the results.

Figure 3 presents the nuclear modification factor R_{CP}: STAR BES-I experimental data are shown in the left panel, UrQMD calculations in the central panel, and SMASH+vHLLE results in the right panel [23].

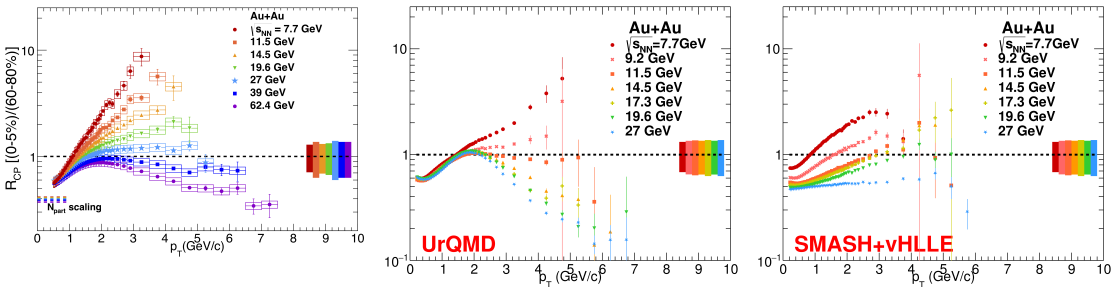

Figure 3: Nuclear modification factor R_{CP} for inclusive charged particles in Au+Au collisions in the energy range $\sqrt{s_{NN}} = 7.7-27$ GeV. Left: STAR experimental data (BES-I). Center: UrQMD simulation results. Right: SMASH+vHLLE simulation results. The error bars represent statistical uncertainties.

4.2 Comparison of Model Predictions with Experiment

The analysis of the obtained model results, when compared with the experimental data, reveals significant differences between the two model approaches depending on the collision energy and the transverse momentum range.

Figure 4 presents a comparison of the nuclear modification factor R_{CP} measured in the STAR experiment (BES-I) with the results of the UrQMD and SMASH+vHLLE simulations for six collision energies in the range $\sqrt{s_{NN}} = 7.7-27$ GeV.

The UrQMD transport model shows good agreement with the experimental data in the low transverse momentum region ($p_T \lesssim 2\text{GeV}/c$), where the suppression of particle production is not yet dominant, for all considered collision energies. In this

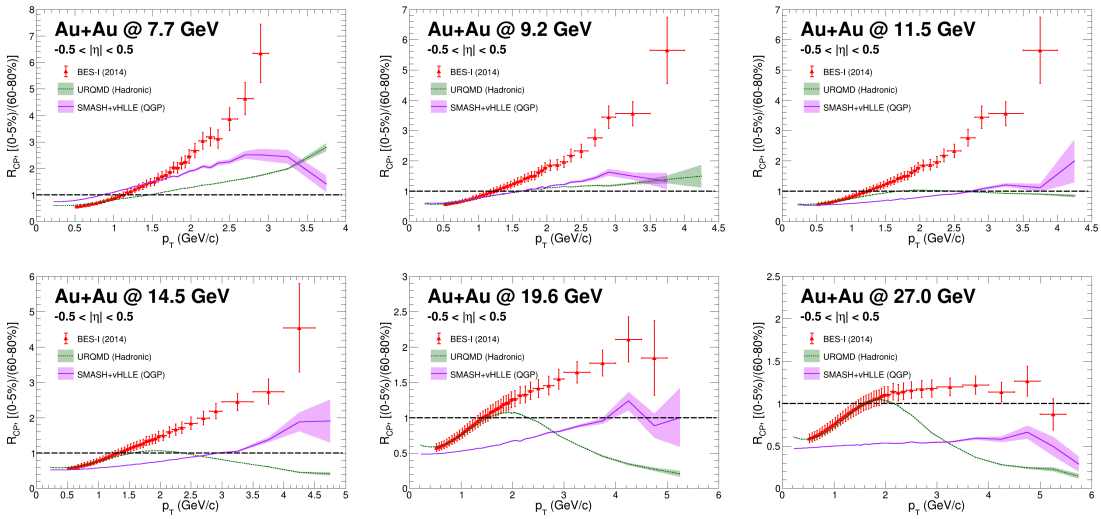

Figure 4: Nuclear modification factor R_{CP} for inclusive charged particles in Au+Au collisions at $\sqrt{s_{NN}} = 7.7 - 27$ GeV. Comparison of STAR BES-I experimental data with calculations from the UrQMD and SMASH+vHLLE models.

range, the model calculations almost coincide with the STAR measurements, indicating a correct description of soft particle production processes within the cascade approach. However, when transitioning to the intermediate and high p_T region, a systematic underestimation of R_{CP} is observed compared to the experimental results. For all energies starting from $\sqrt{s_{NN}} = 11.5$ GeV and above, the UrQMD model predicts an earlier and stronger suppression of particle production compared to the experimental data. In other words, the R_{CP} values in the model begin to decrease at lower transverse momenta than observed in the experiment. For the lowest collision energies (7.7 and 9.2 GeV), the kinematic range is limited to transverse momenta p_T of no more than 4–5 GeV/c, which does not allow a definitive conclusion regarding the presence or absence of suppression effects. In the accessible momentum range, the UrQMD model qualitatively reproduces the trend of the experimental points; however, the quantitative agreement deteriorates with increasing p_T.

The SMASH+vHLLE hybrid model exhibits a fundamentally different behavior of the produced particles within the employed approach. At energies above 11.5 GeV, the model systematically underestimates the nuclear modification factor over almost the entire transverse momentum range, except for the lowest p_T. An underestimation of particle production is observed both in the enhancement region (intermediate p_T) and in the plateau/suppression region. This indicates that the combination of the hydrodynamic description with subsequent hadronization via the cascade leads to a deficit in the production of final-state particles. The most interesting behavior of the SMASH+vHLLE model is observed at the lowest energy $\sqrt{s_{NN}} = 7.7$ GeV. In this case, the hybrid model shows agreement with the experiment up to $p_T \approx 1.2$ GeV/c, practically reproducing the rise of the R_{CP} factor. However, with a further increase in p_T, the model points begin to systematically deviate from the experimental ones, and the discrepancy grows. Such behavior may indicate that at low energies, the hydrodynamic description is applicable only for the softest particles, whereas particles with larger momenta require different production

mechanisms.

The observed differences between the models and the experiment may be due to several factors. For the UrQMD model operating in the purely cascade mode, the overly strong suppression at high p_T suggests an insufficiently accurate description of parton energy loss mechanisms and the absence of collective effects characteristic of a dense medium. The model does not take into account the phase transition to QGM and, consequently, cannot correctly reproduce the full set of properties of dense matter.

For the SMASH+vHLLE hybrid model, the discrepancies, especially at high energies, may be related to the choice of parameters of the hydrodynamic phase, such as the specific shear viscosity η/s, or to the procedure of transitioning from hydrodynamics to the hadronic cascade (hadronization). The partial agreement at $p_T < 1.2$ GeV/c for the 7.7 GeV energy suggests that at low energies the hydrodynamic description of the soft component works satisfactorily, but refinements are needed to describe the hard component of the spectrum.

5 Conclusion

In this work, a comparison was made of the nuclear modification factors R_{CP} for inclusive charged particles in Au+Au collisions in the energy range $\sqrt{s_{NN}} = 7.7-27$ GeV, calculated within the UrQMD and SMASH+vHLLE models, with the experimental data from the STAR experiment obtained in the BES-I program. A unified methodology for calculating R_{CP}, including the use of identical $\langle N_{coll} \rangle$ values from the Glauber model, ensures the validity of the comparison between model and experimental results.

It was shown that the UrQMD transport model reproduces the experimental data well in the low transverse momentum region ($p_T > 2$ GeV/c); however, at higher p_T, it exhibits a stronger suppression of particle production compared to experiment. The SMASH+vHLLE hybrid model, on the contrary, systematically underestimates the R_{CP} values over almost the entire p_T range at energies above 11.5 GeV.

At $\sqrt{s_{NN}} = 7.7$ GeV, the SMASH+vHLLE model shows reasonable agreement with the experimental data in the low p_T region; however, the discrepancies grow with increasing transverse momentum. The obtained results indicate that for a more accurate description of the experimental observations, further optimization of the model parameters and a more detailed account of the physical mechanisms of particle production in the dense nuclear medium are required.

Acknowledgments

This work was supported by the Russian Science Foundation (Grant No. 22-72-10028-P).

Conflicts of Interest

The authors declare no conflict of interest.

References

[1] I. Arsene *et al.* [BRAHMS], Nucl. Phys. A **757**, 1–27 (2005).

[2] J. Adams *et al.* [STAR], Nucl. Phys. A **757**, 102–183 (2005).

[3] K. Adcox *et al.* [PHENIX], Nucl. Phys. A **757**, 184–283 (2005).

[4] B. B. Back *et al.* [PHOBOS], Nucl. Phys. A **757**, 28–101 (2005).

[5] M. Gyulassy and L. McLerran, Nucl. Phys. A **750**, 30–63 (2005).

[6] K. Fukushima and T. Hatsuda, Rep. Prog. Phys. **74**, 014001 (2011).

[7] Y. Aoki, G. Endrodi, Z. Fodor, S. D. Katz, and K. K. Szabo, Nature **443**, 675–678 (2006).

[8] A. Bazavov *et al.* [HotQCD], Phys. Lett. B **795**, 15–21 (2019).

[9] E. S. Bowman and J. I. Kapusta, Phys. Rev. C **79**, 015202 (2009).

[10] S. Ejiri, Phys. Rev. D **78**, 074507 (2008).

[11] J. Adams *et al.* [STAR], Phys. Rev. Lett. **91**, 072304 (2003).

[12] S. S. Adler *et al.* [PHENIX], Phys. Rev. Lett. **91**, 072301 (2003).

[13] B. B. Back *et al.* [PHOBOS], Phys. Rev. Lett. **91**, 072302 (2003).

[14] I. Arsene *et al.* [BRAHMS], Phys. Rev. Lett. **91**, 072305 (2003).

[15] K. J. Eskola, J.-W. Qiu, and X.-N. Wang, Phys. Rev. Lett. **72**, 36–39 (1994).

[16] L. Adamczyk *et al.* [STAR], Phys. Rev. Lett. **121**, 032301 (2018).

[17] M. Bleicher, E. Zabrodin, C. Spieles, S. A. Bass, C. Ernst, S. Soff, L. Bravina, M. Belkacem, H. Weber, H. Stoecker *et al.*, J. Phys. G **25**, 1859–1896 (1999).

[18] S. A. Bass, M. Belkacem, M. Bleicher, M. Brandstetter, L. Bravina, C. Ernst, L. Gerland, M. Hofmann, S. Hofmann, J. Konopka *et al.*, Prog. Part. Nucl. Phys. **41**, 255–369 (1998).

[19] E. L. Bratkovskaya, M. Bleicher, M. Reiter, S. Soff, H. Stoecker, M. van Leeuwen, S. A. Bass, and W. Cassing, Phys. Rev. C **69**, 054907 (2004).

[20] H. Petersen, J. Steinheimer, G. Burau, M. Bleicher, and H. Stöcker, Phys. Rev. C **78**, 044901 (2008).

[21] J. Weil *et al.* [SMASH], Phys. Rev. C **94**, 054905 (2016).

[22] *Web interface for a nuclear overlap calculation code*, available at: `https://web-docs.gsi.de/~misko/overlap/interface.html`.

[23] A. Aitbayev, Universe **10**, 139 (2024).